

Dust Grains in the Interstellar Medium

Section 1: Introduction

In the early visual inspections of the Milky Way by William Herschel more than 200 years ago it was noticed that in some directions we see very few stars. About 110 years later the application of photography to astronomy showed that there are dark regions at some points in the plane of the Milky Way, either due to something hiding the stars behind it or due to a lack of stars in a given direction. For years thereafter the debate about what the dark regions were went on, with the general consensus being that these were actual gaps in the Milky Way. Even in the 1920's, when spiral galaxies beyond our own were looked at and found to have dust lanes in many cases—and so it was suggested that our Galaxy also had such a dust layer in the disk by analogy—the main weight of astronomical opinion was still that space was empty and the observed distribution of globular clusters or stars or galaxies reflected real space distributions. By that time it was mostly accepted that the dark nebulae were due to some type of obscuring material, nature unknown, but these were thought to be local objects.

It was not until 1930 when the idea of what we now call interstellar extinction was fairly convincingly established. Robert Trumpler (1930; *PASP*, **42**, 214) presented a variety of observations supporting the idea that there is a general absorption in space which is concentrated along the plane of the Milky Way, although not necessarily in a perfectly uniform manner. He was able to estimate the general magnitude of the absorption and found that it varies with wavelength. However he attributed the absorption to Rayleigh scattering by gas rather than to dust particles.

Trumpler was studying open clusters and his main evidence for absorption in the ISM came from comparing the estimated distances to these clusters via two methods: one way was to assume that stars of the same spectral type had the same absolute luminosity, leading to relative distances from the observed magnitudes; the other way was to assume that all open clusters have much the same radius in which case the angular sizes of the clusters gives relative distances. Comparing these two estimates, he found that the distances from assuming a constant cluster radius were systematically smaller than those from assuming that the stellar luminosities for a given spectral type is constant, and that the difference grew larger for smaller, fainter clusters. He also noted that the fainter a cluster was the “redder” the continuum of the O and B-type stars were for a given spectral type. These things together implied that either the nature of stars changes with distance or that there was some absorption along the line of sight to these clusters. Trumpler was able to make

a reasonable estimate of the amount of absorption, 0.7 magnitudes per 1000 light years. This approximate value actually has been suggested in 1908 by J. C. Kapteyn so that the Sun is not in a special place in the Milky Way system even though star count statistics suggested this; he then for some unknown reason abandoned this idea 15 years later when he modelled the Galaxy as a relatively small system with the Sun located somewhere close to the center.

Trumpler's paper was by no means the first suggestion of general absorption in space but for whatever reason it represented the turning point in astronomical thought.

Section 1-1: The ISM Extinction Law

Prior to Trumpler's work some people studying dark clouds had shown that the absorption was too strong to be due to Rayleigh scattering, unless the total cloud mass was far larger than it appeared on other grounds. Even then it was suggested that small dust particles could provide the absorption without requiring a large mass.

In the late 1930's through the early 1950's it became clear that there was extinction in the ISM which is not due to Rayleigh scattering. The quantification of the absorption law had to wait for the definition of photometric magnitude systems, rather than the older photographic system. Once this had been done, and extended to the infrared and the ultraviolet, it became clear that the extinction in the ISM is due to small particles with sizes of order $1 \mu\text{m}$, since the absorption varies nearly as $1/\lambda$ for λ values from 0.3 to $2 \mu\text{m}$. Such an absorption is expected when the particle size is similar to the wavelength of the particles.

Studies of the extinction also found a small amount of polarization associated with regions of high absorption, which is another hallmark of solid metallic or dielectric particles. Originally people thought that the dust particles had to be metallic, since they thought that iron meteorites falling to Earth came from interstellar space. Then some calculations of the possible composition of grains were done and people thought that icy particles would be most likely. In either case, the scattering polarization showed that the dust particles are not nice spheres. It is thought that the grains are aligned to some degree by the galactic magnetic field (since the grains are probably dielectrics and thus have a dipole moment which can interact with a magnetic field) so the polarization studies give us one look at the direction of the large scale galactic magnetic field.

In the 1960's when the wavelength range available was extended further into the UV and the infrared, discrete features in the ISM absorption law were discovered: at around $10 \mu\text{m}$ in the IR there is a local feature of strong absorption, and another such occurs at around 2200 \AA in the UV. These features are due to silicates and to some type of graphitic

substance respectively. Figure 37 shows the extinction function in the standard way that it is presented, as a function of $1/\lambda$. This puts a large emphasis on the UV extinction but does show the general rise roughly as $1/\lambda$. The values in the plot are from Rieke and Lebofsky (1985; ApJ, **288**, 618) and Seaton (1979; MNRAS, **187**, 73p).

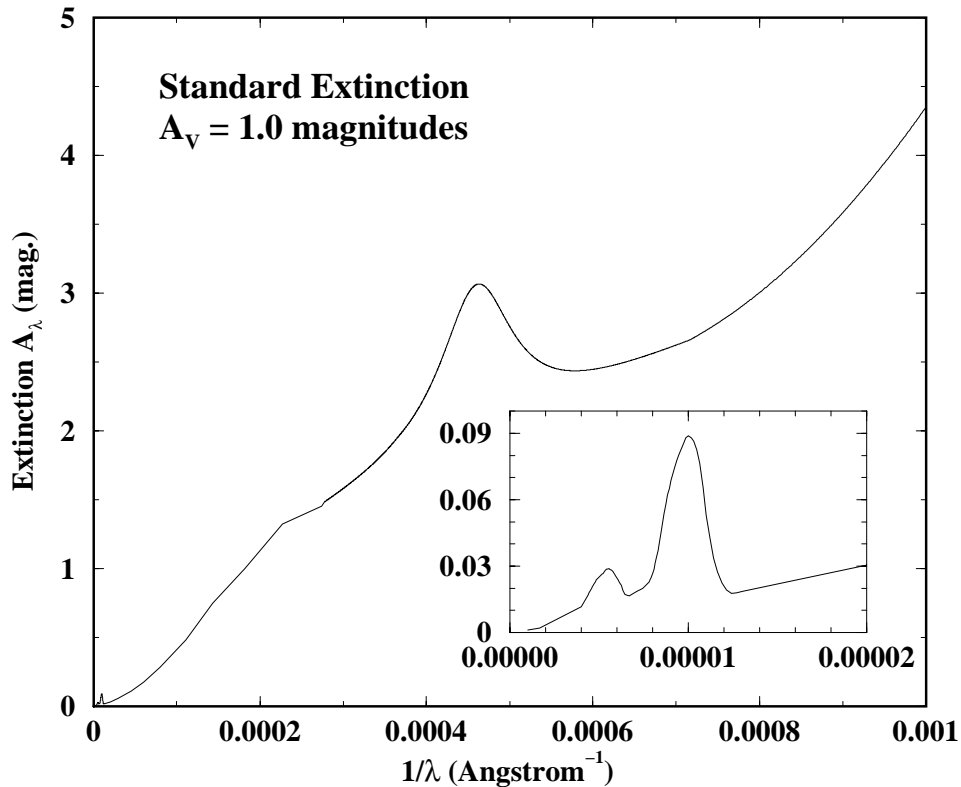


Figure 37—The standard extinction curve from the infrared to the ultraviolet.

Such determinations of the extinction law are due to observations of reddened stars of known spectral type. VI Cyg no. 12 is a prime example of this. The star is a $V = 11.51$ star of type B8Ia, which is subject to about 10 magnitudes of extinction at V . Its colours are $B - V$ of +3.01 and $U - B$ of +1.69 magnitudes compared to expected values of about -0.27 and -1.11 respectively. So it is clear that this star is very heavily reddened. By convention the extinction is given as A_V in magnitudes, and the colour excess $E(B - V) = A_B - A_V$ is also often used for the extinction. The standard value is $A_V = 3.08E(B - V)$. The example star, VI Cyg no. 12 has an A_V value of 9.65 magnitudes and an $E(B - V)$ of +3.28 magnitudes so the ratio there is slightly smaller than the standard value. It is known, in fact, that there are somewhat different extinction functions for different lines of sight, and there has been continued speculation that there is a difference in the extinction in dense clouds compared to the general ISM. In spite of this people normally report either

A_V or $E(B - V)$ and treat them as interchangeable. It is much easier to find $E(B - V)$ or $E(U - B)$ than it is to find the absolute A_V value, since to get A_V we need far-infrared observations while the colour excesses can be derived solely from optical observations.

The ratio $R = A_V/E(B - V)$ is normally 3.1 ± 0.2 for the diffuse ISM, but it appears that it can rise to more than 5 in molecular clouds, presumably because the grains grow larger in the dense gas environment where they can collect material such as ices from the surroundings. The ratio of UV to optical extinction goes down because the small grains are relatively rare in molecular clouds.

There appears to be a good correlation between the extinction $E(B - V)$ and the total hydrogen column density where both of these can be measured. It is thus normally assumed that

$$N_H = 5.9 \cdot 10^{25} E(B - V) \text{ m}^{-2} \quad (5.1)$$

is the relation between the two quantities when they cannot both be measured.

Much work has been done on trying to understand changes in the extinction curve from region to region. The general hypothesis is that there are at least 3 groups of grains contributing to the extinction: there is a population of grains of radius $a \approx 0.1 \mu\text{m}$ which produce the optical extinction; a population of smaller grains $a \approx 0.01 \mu\text{m}$ which produce the far-UV extinction; and the grains which produce the 2200 Å feature which are also small $a \approx 0.01 \mu\text{m}$. From scattering theory (also used for atmospheric physics and thus very well tested) the extinction effect of a particle of radius a will be such that the extinction efficiency parameter Q_{ext} —the total absorption and scattering cross-section σ divided by the geometric cross-section πa^2 —obeys the relation

$$Q_{ext}\lambda = \text{constant} \quad x \lesssim 0.3 \quad (5.2)$$

until the parameter $x = 2\pi a/\lambda$ is of order 0.3, above which the value starts to go down, although the exact way this happens depends on the shape of the grain and whether there is a resonance in the material. When $x \ll 1$ the absorption is proportional to the particle volume while when $x \gtrsim 1$ it becomes proportional to the surface area. By the way, when a particle is not spherical a is some typical dimension of the particle but is difficult to define explicitly. People therefore pretend that the grains are spherical for defining the Q value.

The reason we deduce the existence of 3 grain populations is that the 2200 Å bump, the far UV extinction, and the optical extinction are observed to each change without effecting the other components. The grains producing the UV extinction at less than 2500 Å must have a values a few times smaller than this for the x parameter to be rather smaller than 1, else we would be able to observe the turnover as x comes near the limit of the general

$Q_{ext}-\lambda$ relation given above. So these grains are thought to be small, say $a \sim 0.01 \mu\text{m}$. On the other hand it seems that the optical extinction has to be produced by larger particles than this because the extinction curve does appear to be starting to flatten out in the far blue or near UV before the 2200 \AA feature is encountered. This implies grains of radius $0.15 \mu\text{m}$ or so, larger than those that produce the far-UV extinction. If only the $0.15 \mu\text{m}$ grains were present, we would expect the extinction values at $\lambda < 2000 \text{ \AA}$ to be more or less constant, which is not what is observed.

To refine this somewhat speculative discussion, the detailed theory of how such small grains interact with radiation has to be used.

Section 1-2: Optical Properties of Grains

Whole books have been written about the optical properties of small particles, and their absorption and scattering characteristics. What is useful here is that each dust grain has an effective cross-section

$$C_{\text{ext}}(\lambda) = Q_{\text{ext}}(\lambda)G \quad (5.3)$$

where G is the geometrical cross-section of the grain. For spheres of radius a this is πa^2 . The Q_{ext} value can be split into absorption and scattering parts,

$$Q_{\text{ext}}(\lambda) = Q_{\text{abs}}(\lambda) + Q_{\text{scat}}(\lambda) \quad (5.4)$$

and these both contribute to the total optical depth for a set of grains along our line of sight to some object

$$\tau_{\lambda} = \int_0^{\infty} N(a)\pi a^2 Q_{\text{ext}} da \quad (5.5)$$

where $N(a) da$ is the column density of grains along the line of sight with radius values between a and $a+da$. This $N(a)$ function depends upon the grain size distribution function, the number of grains per unit volume at different points along the line of sight, and the distance to the object. If we assume that there is a constant distribution of grain sizes $p(a)$ at all points in the ISM (which is a rather drastic assumption, but which serves as a starting point for discussion) then I can write

$$\tau_{\lambda} = \int_0^{r_0} \left[\int_0^{\infty} p(a)\pi a^2 Q_{\text{ext}}(a) da \right] N_d(r) dr \quad (5.6)$$

for the optical depth to distance r_0 . In this equation $N_d(r)$ is the total number density of grains at each point for our line of sight. The quantity in the square brackets is a function

of the grain properties, by assumption not a function of r . If I put

$$N_d(\text{total}, r_0) = \int_0^{r_0} N_d(r) dr \quad (5.7)$$

then I have that

$$\tau_\lambda = N_d(\text{total}, r_0) \int_0^\infty p(a) \pi a^2 Q_{\text{ext}}(a) da \quad (5.8)$$

subject to

$$\int_0^\infty p(a) da = 1 \quad (5.9)$$

because $p(a)$ is a probability function. The optical depth is just the ratio of the area blocked by all the dust particles to the cross-section A of the volume Ar_0 of space in which the $N_d(\text{total}, r_0)$ is calculated. If we choose A to be of unit area, then N_d is the normal number density of dust grains. Given a long enough path length the τ_λ value can be larger than 1.

As noted briefly in the previous section, the Q_{ext} value is a function of wavelength. It can be calculated, for a given shape, from the index of refraction of the material. This is normally given in complex form $m(\lambda) = n(\lambda) - ik(\lambda)$, in which the complex part produces a phase shift, by a calculation from classical electromagnetism. For spheres the equations have exact solutions, but for arbitrary shape general solutions are not known. People can carry out numerical approximations for general shapes but such calculations are time consuming.

Section 1–3: Mie Theory

The solution to Maxwell's equations for a sphere of given m value can be found in closed form. This is discussed in various books about optics and electromagnetic field theory. The book *Light Scattering by Small Particles* by H. C. van de Hulst presents the full range of solutions that are known. In the case of spherical grains the original development was by A. N. Mie, *Ann.Physik*, **25**, 377, (1908). The scattered wave can be expressed in spherical harmonics in angle times a spherical Bessel function in radius. Using the boundary conditions of electromagnetism a full solution can be found for all space, within the grain and outside it. One is able to calculate the Q values from the coefficients of the various spherical harmonics.

The scattering efficiency is in general a function of the angle θ between the original direction of wave propagation and the direction that the wave is scattered. For spherical

particles there is no change in the scattering properties with the polarization of the incoming radiation. Although the exact angular distribution can be derived, it is more common to express the average angular distribution by calculating

$$\overline{\cos \theta} = \frac{\int_0^\pi I(\theta) \cos \theta \sin \theta d\theta}{\int_0^\pi I(\theta) \sin \theta d\theta} \quad (5.10)$$

in which $I(\theta)$ is the intensity of scattered radiation at an angle θ . There is no ϕ dependence of the scattering, since the problem is totally symmetric in the ϕ coordinate. Values of the $\overline{\cos \theta}$ quantity can be between -1 and $+1$. It is zero for isotropic scattering, -1 when all the scattering is back along the original ray direction, and $+1$ when all the scattering is forward along the original ray direction.

The formulae that result are as follows. For a grain of radius a and a wavelength λ , having index of refraction $m = n - ik$ the variables that appear in the solution are

$$x = \frac{2\pi a}{\lambda} \quad \text{and} \quad y = mx \quad (5.11)$$

in terms of which

$$\begin{aligned} Q_{\text{ext}} &= \frac{2}{x^2} \sum_{j=1}^{\infty} (2j+1) \left[|a_j|^2 + |b_j|^2 \right] \\ Q_{\text{scat}} &= \frac{2}{x^2} \sum_{j=1}^{\infty} (2j+1) [\text{Re} \{a_j + b_j\}] \\ Q_{\text{abs}} &= Q_{\text{ext}} - Q_{\text{scat}} \\ Q_{\text{abs}} \overline{\cos \theta} &= \frac{4}{x^2} \sum_{j=1}^{\infty} \frac{j(2j+1)}{j+1} \text{Re} \{a_j a_{j+1}^* + b_j b_{j+1}^*\} + \frac{4}{x^2} \sum_{j=0}^{\infty} \frac{2j+1}{j(j+1)} \text{Re} \{a_j b_j^*\} \end{aligned} \quad (5.12)$$

with complex coefficients a_j and b_j . These are the coefficients of the spherical harmonics; the wave produced by the interaction with the grain is described by two scalar functions from which the \vec{E} and \vec{H} fields are derived. These functions, u and v , are given by

$$\begin{aligned} u &= e^{i\omega t} \cos \phi \sum_{n=1}^{\infty} -a_n (-i)^n P_n^1(\cos \theta) h_n^{(2)}(kr) \\ v &= e^{i\omega t} \sin \phi \sum_{n=1}^{\infty} -b_n (-i)^n P_n^1(\cos \theta) h_n^{(2)}(kr) \end{aligned} \quad (5.13)$$

with $k = 2\pi/\lambda$, (r, θ, ϕ) as the usual spherical coordinates, and $h_n^{(2)}$ being the spherical Bessel function of the second kind of order n .

The expansion coefficients can be found from the equations

$$\begin{aligned}
 a_j &= \frac{\left[\frac{A_j(y)}{m} + \frac{j}{x}\right] \operatorname{Re}\{\alpha_j(x)\} - \operatorname{Re}\{\alpha_{j-1}(x)\}}{\left[\frac{A_j(y)}{m} + \frac{j}{x}\right] \alpha_j(x) - \alpha_{j-1}(x)} \\
 b_j &= \frac{\left[mA_j(y) + \frac{j}{x}\right] \operatorname{Re}\{\alpha_j(x)\} - \operatorname{Re}\{\alpha_{j-1}(x)\}}{\left[mA_j(y) + \frac{j}{x}\right] \alpha_j(x) - \alpha_{j-1}(x)}
 \end{aligned} \tag{5.14}$$

and the recurrence relations

$$\begin{aligned}
 \alpha_j(x) &= \frac{2j-1}{x} \alpha_{j-1}(x) - \alpha_{j-2}(x) \\
 A_j(y) &= -\frac{j}{y} + \frac{1}{\frac{j}{y} - A_{j-1}(y)}
 \end{aligned} \tag{5.15}$$

with the starting values $A_0(y) = \cos(y)/\sin(y)$, $\alpha_{-1}(x) = \cos(x) - i\sin(x)$, and $\alpha_0(x) = \sin(x) + i\cos(x)$.

The index of refraction is found from

$$m^2 = \frac{\varepsilon(\omega)}{\varepsilon_0} - i \frac{\sigma(\omega)}{\omega\varepsilon_0} \tag{5.16}$$

where ε is the dielectric constant and σ is the conductivity, both at the specific frequency ω under consideration. From this the n and k values can be found. In many cases m^2 appears in the formulae so the original values from this last equation can be used directly. Note that it is not sufficient to use the optical index of refraction at other frequencies, nor can one use the static dielectric constant or conductivity in this formula.

Notice that everything is determined by x for a given index of refraction. If the m value were constant, then all particles of the same a/λ will yield exactly the same Q values and $\overline{\cos\theta}$ value.

The limiting values of these expansions can be found in two limits. First, when x is small (that is, the particle is small compared to the wavelength) and also mx is small (which will normally be the case for dielectric materials, but not always for metallic grains) the general results are

$$\begin{aligned}
 Q_{\text{ext}} &= -\operatorname{Im} \left\{ 4x \frac{m^2-1}{m^2+2} + \frac{4}{15} \left(\frac{m^2-1}{m^2+2} \right)^2 \frac{m^4+27m^2+38}{2m^2+3} \right\} \\
 &\quad + x^4 \operatorname{Re} \left\{ \frac{8}{3} \left(\frac{m^2-1}{m^2+2} \right)^2 \right\} \\
 Q_{\text{sca}} &= x^4 \frac{8}{3} \left| \frac{m^2-1}{m^2+2} \right|^2
 \end{aligned} \tag{5.17}$$

and the scattering becomes isotropic for these small grains. If the m value is not changing much with x then the scattering goes as λ^{-4} as is the case for Rayleigh scattering. For realistic m values the dependence can be much different than the Rayleigh case. Indeed most grain materials of interest in astronomy have relatively little scattering at long wavelengths.

In the limit that the grain is large compared to the wavelength then the Q values become constant. The asymptotic values are

$$Q_{\text{ext}} = 2 \quad Q_{\text{scat}} = 1 + w \quad Q_{\text{abs}} = 1 - w \quad (5.18)$$

in which w is the albedo of the grain. This is 1 for pure scattering and 0 for pure absorption. It is not possible to give a simple general formula for w from the index of refraction. Note that the total Q_{ext} value is 2 when the grain is large compared to the radius, not 1 as might be thought. If the grain is very large it is likely that all the radiation will be absorbed in trying to pass through it, so then it certainly absorbs with its geometrical cross-section πa^2 . Then it must have scattering at the surface, which contributes another πa^2 to the cross-section, for scattering in all possible directions. If there is more scattering from the surface regions the albedo goes up. Even in the pure absorption case there must be some scattering right at the surface so calling the $w = 0$ case “pure absorption” is slightly misleading.

Figure 38 shows an example of the results of Mie theory. I have calculated the Q values for $n = 1.33 - 0.1i$ and a of $0.5 \mu\text{m}$. You see that there is an initial rise in Q_{ext} to $a/\lambda \sim 1$ after which the curve turns over and goes to a local minimum before settling down to a nearly constant value. The local maximum and minimum values are due to resonances in the waves going through the grain, and are all due to the scattering part rather than the absorption part. I also show the $\overline{\cos\theta}$ values for different a/λ values. There is strong forward scattering for $x \sim 1$, but not much asymmetry for either very large or very small x values.

If the grains have different sizes the resonances are smoothed out. This is shown in Figure 39 where I use the same m value but put in a distribution of sizes between 0.1 and $0.7 \mu\text{m}$, such that the average size is $0.1589 \mu\text{m}$. Now I show the results as a function of $1/\lambda$ since for each value there will be a range of x values used in the Mie calculations. The Q values are now with respect to the mean a value, so they turn out to be somewhat higher than what is found for grains of a single radius. The vertical dashed line shows where $\langle a \rangle / \lambda$ is 1.

One thing that is a bit different in Figure 39 compared to the single size case is that the $\overline{\cos\theta}$ value is usually different than 0. At longer wavelengths there is significant forward scattering while at shorter wavelengths there tends to be some backscattering.

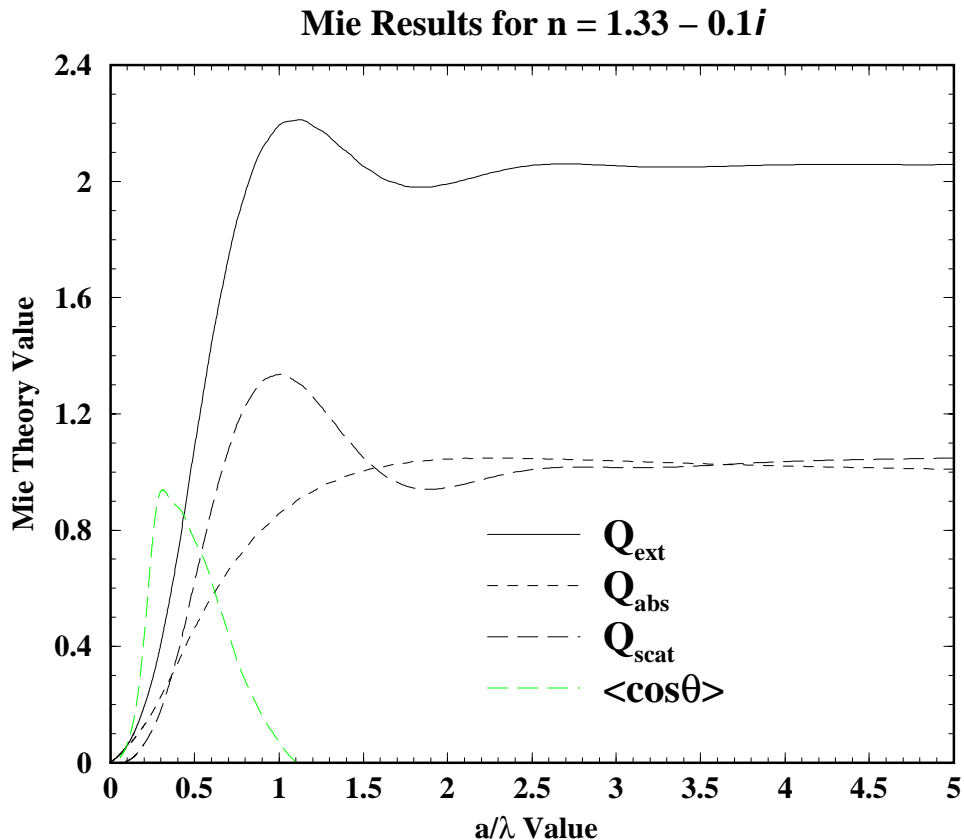


Figure 38—The results of Mie theory for grains of size $0.5 \mu\text{m}$ and $m = 1.33 - 0.1i$.

All of these results are for a constant m . When the wavelength dependence of m is included distinctly different results can be found. Figure 40 shows the results of Mie theory for silicate grains made up of Forsterite, a common type of silicate material on Earth, allowing for the $m(\lambda)$ function, for a radius of $0.5 \mu\text{m}$.

With the m value being a function of wavelength, there is more structure in the Q curves. For this particular material there is a lot of scattering and only a little absorption for most wavelengths. Only for $a/\lambda > 2$ is there much absorption. That means that $\lambda < 2500 \text{ \AA}$ is needed to get strong absorption: the grain material is a glassy substance, and is fairly transparent for optical or longer wavelengths at this size. At long wavelengths there are two features due to internal resonances in the Si–O bonds of the material. This is shown in Figure 41. These features, at 10 and $18 \mu\text{m}$, are commonly observed in infrared spectra of dusty objects including late-type stars with circumstellar shells and dusty HII regions.

Figure 42 shows the actual n and k functions for Forsterite. The n value has a peak in the short wavelength UV, is fairly flat from the optical range to the near-infrared, and has a discrete feature at around $10 \mu\text{m}$. The k part is small for the optical and near-infrared

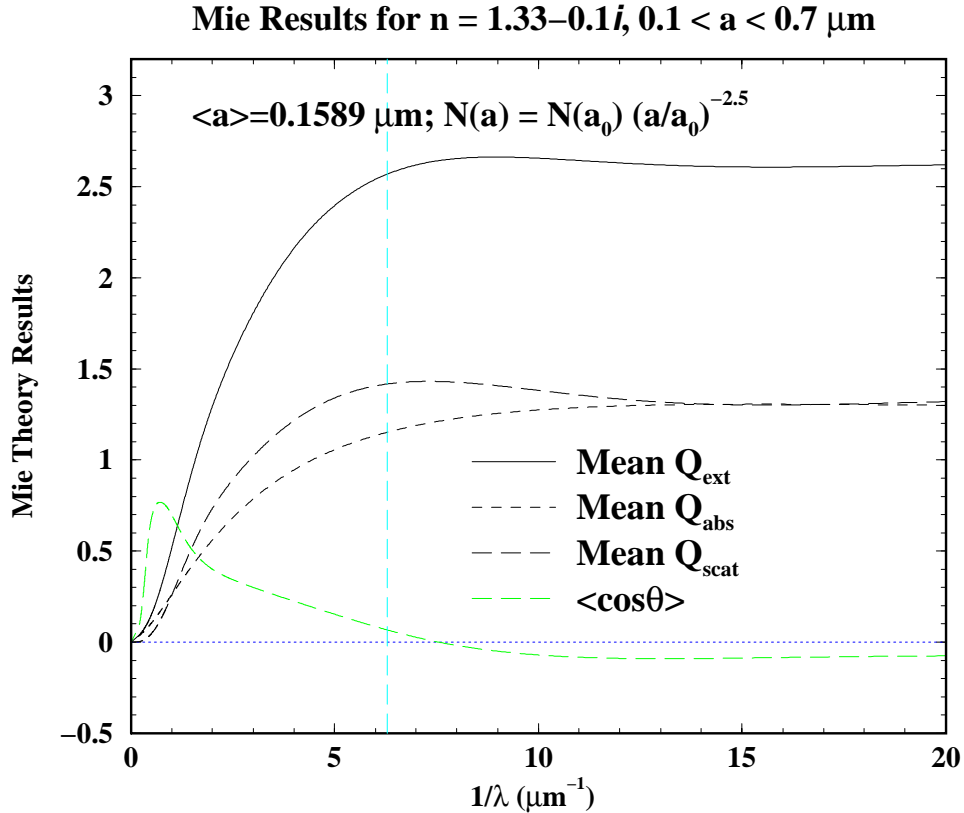


Figure 39—The results of Mie theory for a range of grain sizes from 0.1 to $0.7 \mu\text{m}$ and $m = 1.33 - 0.1i$.

wavelength ranges, but is significant in the far-infrared. It is the interplay between n and k that produces the two features in the far-infrared. One cannot deduce the nature of the features from either quantity alone.

When a range of grain sizes are present, most of the short wavelength structure disappears as is seen in Figure 43. The long wavelength features are due primarily to the m terms and not to the functions of x , hence they are the same for all a values and appear in the mean Q curves. Here I have assumed a distribution of a values from 0.05 to $1 \mu\text{m}$ with a size distribution $N(a) \propto a^{-3.5}$, so the average a value is $0.0824 \mu\text{m}$. Now the Q values rise until $\bar{x} \approx 2.6$ and then the Q_{scat} value decreases and all the Q values become nearly constant. The turn-over occurs when the smallest grains have a/λ of 0.25 . This is somewhat different than what is expected on general terms for grains of a given size, where the turn-over occurs at $x \sim 0.3$ or $a/\lambda \sim 0.05$. The reason for this difference is that there is a strong change in $m(\lambda)$ in the UV.

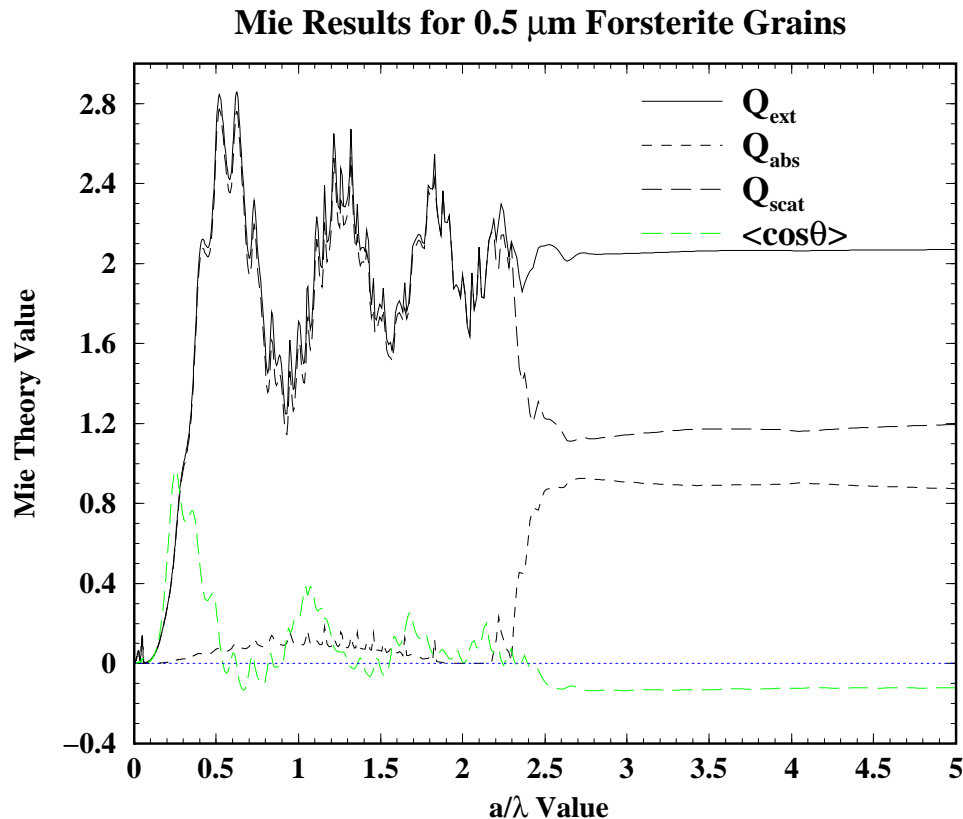


Figure 40—The results of Mie theory for Forsterite grains of radius 0.5 μm .

If the dust particles are not spherical and are aligned in some way then there is a net polarization produced by scattering, since the scattering efficiency is different for radiation polarized along the long axis of the particles compared to that polarized along the short axis of the particles. The scattering is somewhat more efficient for the polarization along the short axis, say of a cylindrical grain, so after a certain path length in the ISM with grains oriented in a particular direction the starlight has a small residual polarization whose direction is perpendicular to the grain orientation direction as defined by the long axis.

This type of polarization is observed in reddened early-type stars, and the degree of polarization increases with the $E(B - V)$ value. At a distance of 1 kpc, a typical value is 3% linear polarization in the visible range. The degree of linear polarization is a function of wavelength and is generally approximated by

$$\frac{p(\lambda)}{p_{\text{max}}} = e^{-1.15 \ln^2(\lambda_{\text{max}}/\lambda)} \quad (5.19)$$

with λ_{max} somewhere in the range 4500 to 8000 \AA , mostly close to 5500 \AA . Variations in

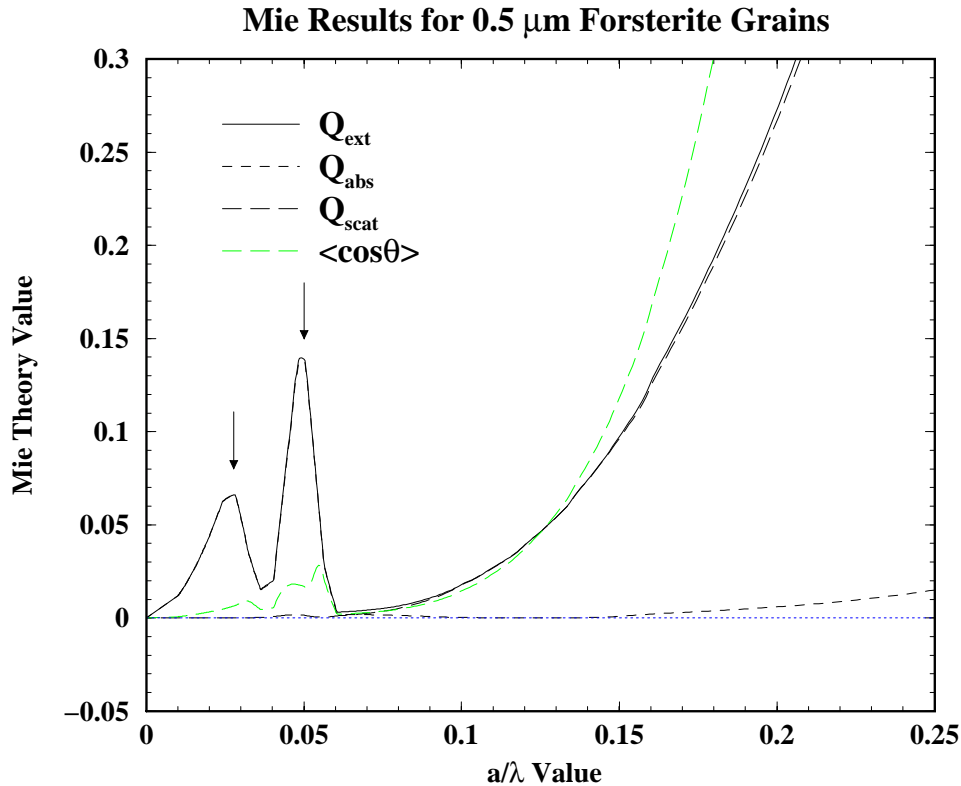


Figure 41—The results of Mie theory for Forsterite grains of radius $0.5 \mu\text{m}$, showing the far-infrared features at 10 and $18 \mu\text{m}$. These features can be seen in the extinction curve, and are also observed in various cool stars with circumstellar dust shells.

λ_{max} are correlated with variations in the $A_V/E(B-V)$ ratio, and thus indicate variations in the grain properties for different lines of sight.

The grains that produce this linear polarization also produce circular polarization. Observations of intrinsically polarized sources show this effect best, but it can also be observed for normal stars. The degree of circular polarization is small and thus it is difficult to detect with sufficient accuracy to deduce details of the grain properties.

People have studied these extinction effects to deduce what the grains are like. The grains need to be non-spherical and have some systematic alignment. It appears that the polarization is small in the ultraviolet and so the small grains that produce the UV extinction are either spherical or are not aligned. The grains that produce the optical extinction are aligned, and it is thought that this is due to the galactic magnetic field. The characteristics of the polarization seem to suggest that the grains are dielectric (rather than metallic) and that their a value is of order $0.3 \mu\text{m}$.

The observations of this polarization are more valuable as tracers of the galactic magnetic field than as a probe of the dust particles. It is thought that the direction of the linear

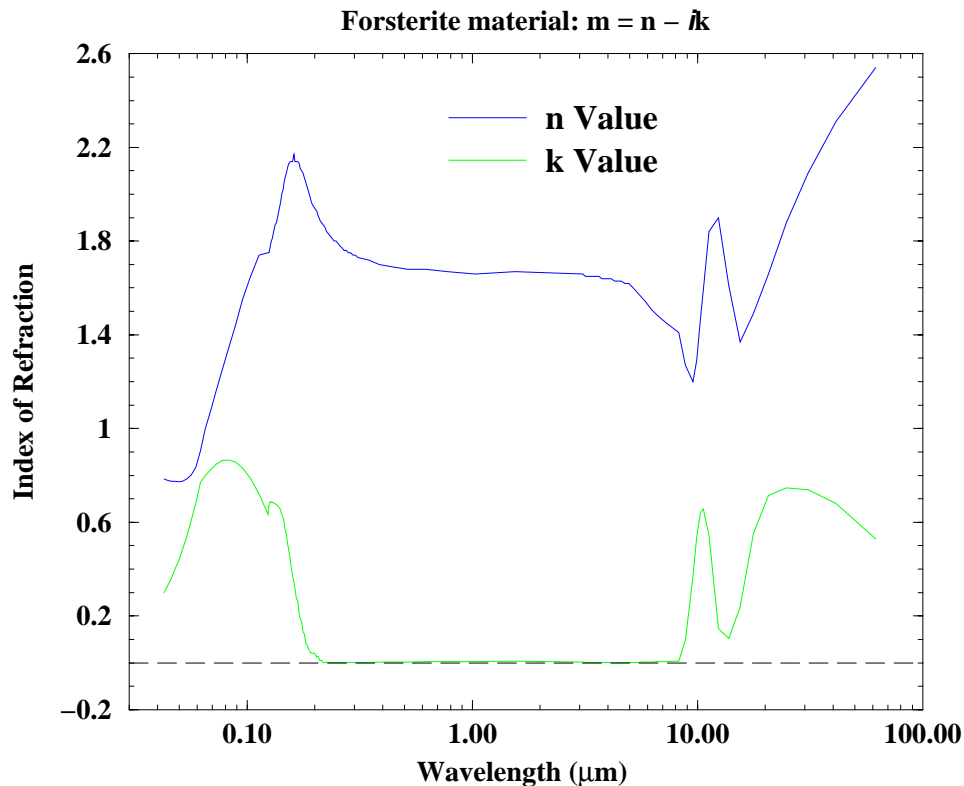


Figure 42—The measured m and k values for Forsterite silicates.

polarization vector is along the local magnetic field. It is likely that the grains are both charged and rotating, hence they will have both electric and magnetic dipole moments. Such grains can interact strongly with a relatively weak magnetic field. The magnitude of the galactic \vec{B} field is a few micro-gauss, but that still is enough to align the grains under the relatively low temperature conditions of the ISM. If the grains are given random rotational angular momentum and this is then re-distributed in collisions, it is expected that the general net rotation will tend to be along the axis of largest moment of inertia: for cylindrical or ellipsoidal grains, this is an axis along the short dimension of the grain. This is also where the axis where the excess polarization is produced by scattering. The end result is that the polarization vectors observed are expected to show the direction of the magnetic field.

Section 2: General Grain Properties in the ISM

There have been many attempts to derive the grain properties for the ISM from the available observations. The constraints are the observed wavelength dependence of A_λ , the relation between A_V and the hydrogen column density, polarization measurements,

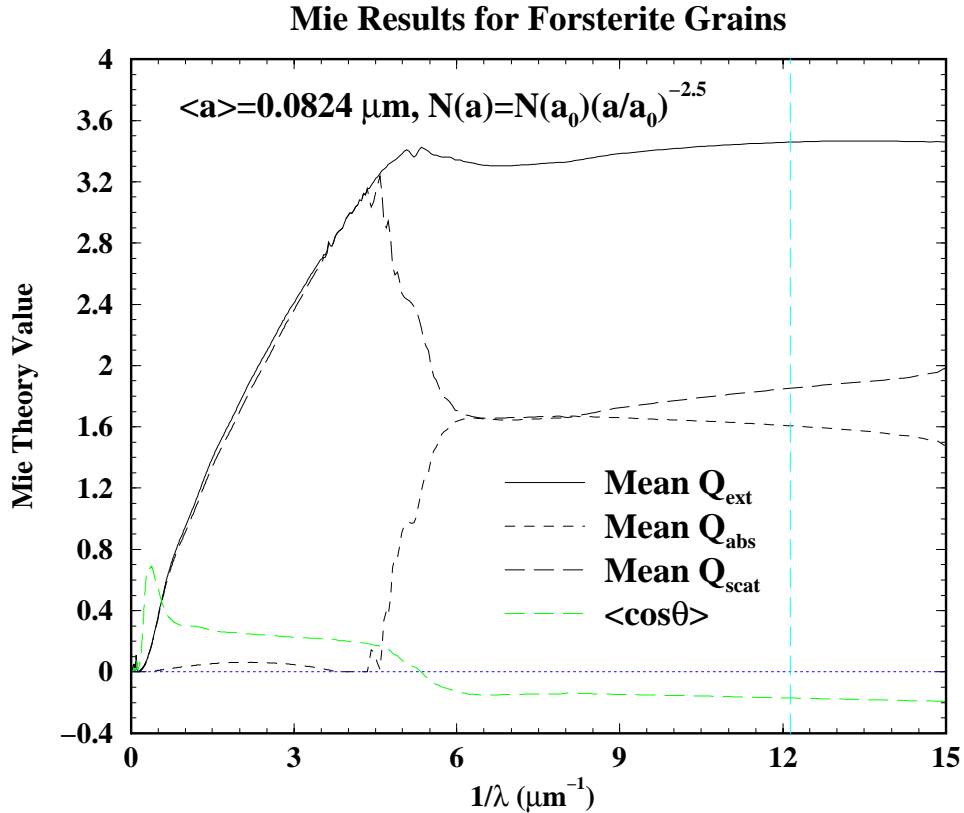


Figure 43—The results of Mie theory for Forsterite grains of with radii between 0.05 and 1.0 μm , with a weighting function $N(a) = N(a_0)(a/a_0)^{-3.5}$. Most of the fine structure from Figure 41 is removed by having a size distribution, but note that the 10 and 18 μm features are still present.

and general abundance properties observed in the ISM. We know that in the general ISM some elements, particularly Mg, Si, and Fe, are depleted compared to the “standard” cosmic abundances. Only about 2% of these elements are in the gas phase of the ISM outside of molecular clouds. The CNO elements are also somewhat depleted: O by about 25%, and C and N by about 80%.

Given the observed depletions we can check on whether some types of grains can produce the observed $E(B - V)$ to N_H relation. One finds that if all the Si goes into quartz the extinction that would be produced is smaller than what is observed by a factor of 3, and the same is true for any known silicate material. However if the depleted O alone goes to ice particles, they would provide more than enough material to produce the observed extinction. Thus it is thought that the CNO elements somehow produce much of the extinction, probably by forming ice coatings on silicate or iron-based core grains. This is not at all surprising under the low temperature conditions of the ISM (although, as usual

when a system is far from thermodynamic equilibrium, we have to be careful in speaking about the temperature of the ISM).

Once infrared observations became available for some heavily obscured stars, it was found that they show strong absorption bands due to the H–O bond in water at $3.1 \mu\text{m}$ and due to Si–O bond in silicates at 10 microns. This fits with the picture of a silicate core grain with a water ice coating. Actually it is likely from a chemical standpoint that the ice material includes CH_4 , NH_3 , and H_2O . It is thought that the silicate grains ejected from late-type giant stars form nucleation centers; once they cool to a temperature of the order of 10 K in the ISM, the more volatile icy materials can condense into them to make the typical grains of the ISM. In the general ISM there is sufficient radiation that the gas is more in atomic than molecular form, and a complex chemistry is probably going on all the time on the grain surfaces. In this case the ices probably form directly on the grain surface, rather than forming in the gas first and then condensing onto the grains. Such evidence as we have suggests that the icy mantle is typically 60% water ice by mass.

We now also have evidence that some CO condenses onto the grains in molecular regions, since this is the likely to be the most abundant molecule aside from H_2 . Solid CO produces a band at $4.675 \mu\text{m}$ which is distinct from the fundamental CO vibrational band. Different molecular clouds show different relative strengths of the H_2O and solid CO bands, reflecting different physical conditions and histories of the grains. The CO/ H_2O ratios vary from small values up to about 0.3 in different objects.

In some regions there is clearly no water ice on the grains, since there is no $3.1 \mu\text{m}$ absorption observed despite a large A_V . In these cases it is thought that the mantle around the core grain is not due to water ice, but due to some combination of the CNO elements. Observations have shown that there is some type of carbon-based mantle material which produces the UIR features, since these can be observed in absorption towards heavily reddened stars. This was first seen at $3.4 \mu\text{m}$ for lines of sight towards the galactic center.

Section 2–1: Equilibrium Grain Temperatures

If a grain has known Q values it is possible to calculate the expected temperature in the ISM by calculating the temperature where heating and cooling balance. The emissivity of a single (spherical) grain is given by

$$\varepsilon(\nu) = \pi a^2 Q_{\text{abs}}(\nu) B_\nu(T_d) \quad (5.20)$$

for dust grains of temperature T_d . The total energy absorbed at frequency ν is given by

$$a(\nu) = 4\pi J_\nu Q_{\text{abs}}(\nu) \pi a^2 \quad (5.21)$$

with some local mean intensity of the radiation field J_ν . Note that in both cases only Q_{abs} contributes to the heating or cooling. A global balance of heating and cooling requires that

$$\int_0^\infty Q_{\text{abs}}(\nu) B_\nu(T_d) d\nu = \int_0^\infty Q_{\text{abs}}(\nu) J_\nu d\nu \quad (5.22)$$

which applies at each radius a . Different size grains will have different T_d values in most cases.

In finding a T_d value we get only the equilibrium temperature of the grains. Since the radiation field of the ISM is quite diffuse, and since it is formed of individual photons, the actual grain temperature may fluctuate around T_d : it goes up when a UV photon is absorbed, falls as the grain cools, and the time average temperature is T_d . As the grains get smaller the deviations from T_d get larger, since the energy of a single photon is a larger fraction of the total thermal energy of the grain.

An example of how this works is shown in Figure 44 where I take a case of a small grain (a of $0.02 \mu\text{m}$) in a radiation field which matches a highly diluted 10^4 K blackbody. I assume that the grain has a minimum temperature of 1.5 K due to collisions with gas particles and the effect of the 2.7 K cosmic background radiation. When a photon from the diffuse radiation field is absorbed the grain gains energy, and its temperature increases. It then cools off back towards the minimum temperature until another photon is absorbed. One has to assume a relation between the internal energy of the grain and the temperature to do this type of calculation.

The general feature of the $T(t)$ function illustrate why the average temperature (shown by the dashed line) cannot be used to accurately predict the emission. The energy radiated goes roughly as T^4 . When the grain is hot it radiates a lot of energy. Most of the time it is cooler than the long-term average temperature and does not radiate much energy. Since the emission from the grain at a temperature of 15 K is not only more intense than what results when the grain is near the minimum temperature but also extends to much shorter wavelengths, the practical difference in the resulting spectrum is quite dramatic.

I show a few temperature spikes in detail in Figure 44b. The process is random so there is sometimes the absorption of a second photon while the grain is still cooling off from a previous absorption. The time interval between absorptions and the photon energy of an absorption vary in a random manner as well.

If I repeat the same calculation with a large grain, say a of $1 \mu\text{m}$ then the situation shown in Figure 45 results. The total energy of the grain is much larger—it goes as a^3 —and the temperature changes for any photon being absorbed is rather small. Due to the larger cross-section of the grain the photons are absorbed more frequently than in the

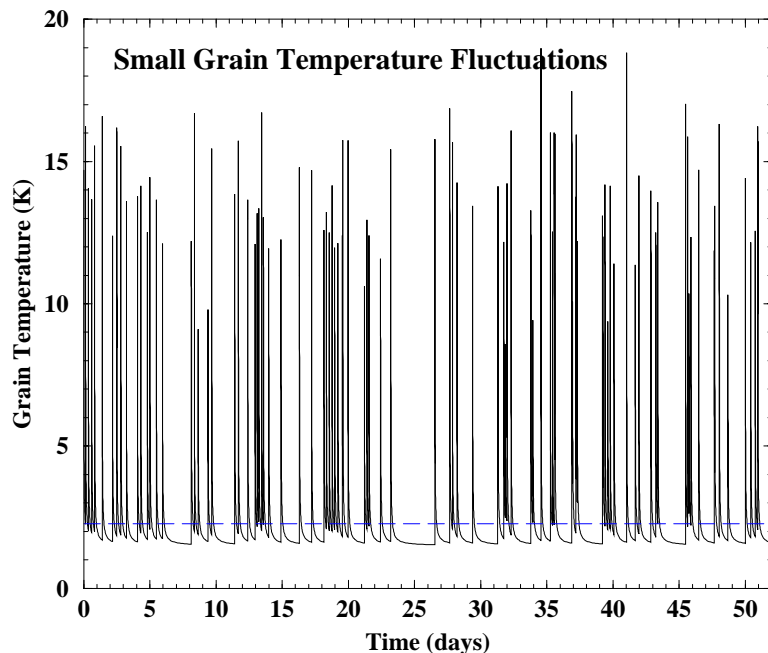


Figure 44a—A simulation of the effect of transient heating in a very small grain. Here I have carried out a simulation of the random absorption of photons from a dilute radiation field by a grain of radius $0.02 \mu\text{m}$. The grain is assumed to have a minimum temperature of 1.5 K determined by other sources of heating aside from the radiation from the ISM radiation field. The dashed line shows the average temperature that the balance of heating and cooling would predict.

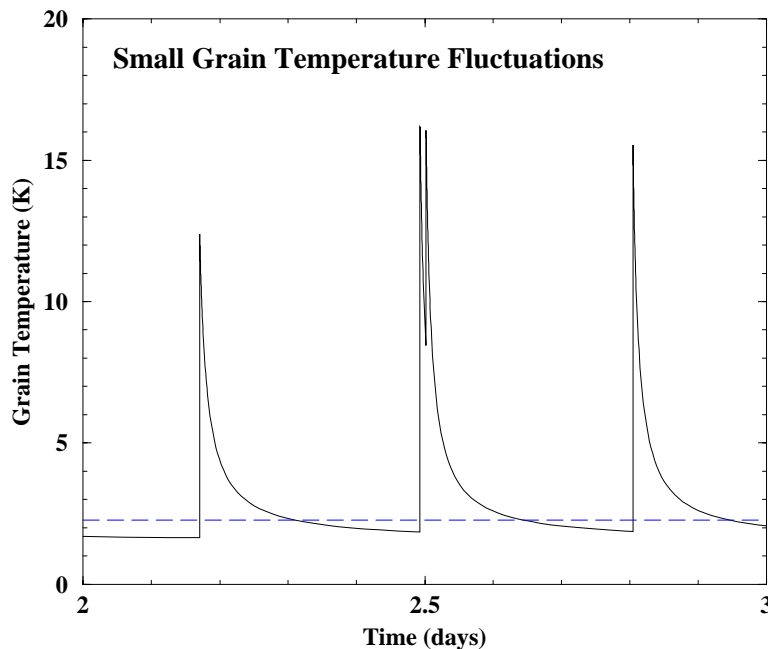


Figure 44b—A close up of a few of the random heating events.

previous example. Photons are absorbed every few seconds, rather than every few hours. The fluctuations are small and so the average temperature gives the proper amount of radiation.

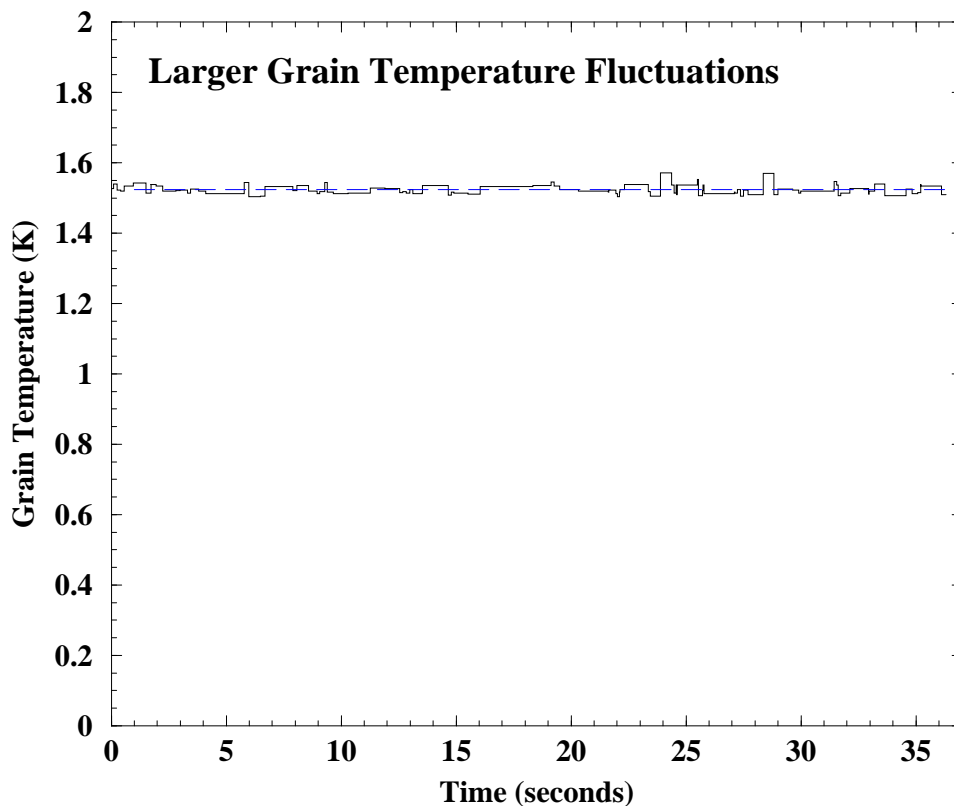


Figure 45—The results of the random photon absorption calculation for a grain of radius $1.0 \mu\text{m}$ under the same conditions as in Figure 44 above. For this large grain the temperature fluctuations are small and the mean temperature can be used to accurately calculate the emission.

Section 2-2: The 2200 \AA Feature

The large peak in the ISM extinction curve at around 2200 \AA was only discovered in the 1960's, since it requires space observations. The wealth of data from the *International Ultraviolet Explorer* satellite (IUE) has given us lots of data about the extinction in this feature. The peak of the feature is actually at 2175 \AA and that value seems to be constant to the limits of the accuracy of the observations. There are small changes in shape over different lines of sight, which are mostly due to variations of the feature width by up to 10%

The most common explanation of the 2175 \AA peak is that it is due to small graphite

grains. Graphite has a strong resonance in the ultraviolet due to the valence electrons in π -orbitals, which can match the observed feature. Another point in favour of this idea is that carbon stars produce large amounts of carbon-rich dust, so there is a source for such grains. There are problems with this idea however, since the band shape and position are likely to be sensitive to the exact size and shape of the grains whereas the observed feature is quite uniform. Graphite has a complicated non-isotropic dielectric constant, so it is not possible to apply normal Mie theory to such grains even if they are spherical. It has also been suggested that graphite grains will not last for long periods of time in the ISM since they have very reactive surfaces, and are predicted to be destroyed by chemical processes as carbon atoms are removed from the surface.

There have been other suggestions of the cause of the 2175 Å peak, such as the hypothesis that it is due to Mg_2SiO_4 grains with some contamination by OH^- radicals (T. M. Steel and W. W. Duley, 1987; ApJ, **315**, 337). None of these is clearly favoured at the present time.

It is also possible to look at the UV extinction in the Magellanic Clouds, which have lower metallicities than does the Galaxy. The main problem in doing this is that the internal extinction in the clouds is relatively small, only of order 0.3 in $E(B - V)$. The optical extinction function is similar to what is observed in the Galaxy, including the linear polarization properties. The UV extinction is quite anomalous by comparison. In some parts of the SMC it seems that the 2200 bump is entirely absent. In other parts the UV extinction is similar to that in the Galaxy. Where the 2200 Å bump is missing the far-UV extinction is much higher relative to the V extinction than in the Galaxy. The LMC has an intermediate type of extinction function between that in the SMC and that in the Galaxy. It seems that the small grains that produce the galactic far UV extinction are different in the SMC and LMC than in the Galaxy. Further, the weakness of the 2200 Å bump seems to be correlated with the C/O ratios of the clouds, which would support the idea that the grains producing this feature are carbonaceous in nature. The larger ratio of far-UV to optical extinction indicates a relatively larger fraction of small grains in the clouds compared to the Galaxy.

It is also clear that the A_V/N_H ratios of the clouds are smaller than that in the Galaxy, by about a factor of 4 in the LMC and by a factor of 20 in the SMC. These decreases follow the total N_{CNO}/N_H ratio, so it appears that the availability of these elements directly changes the population of large grains.

Section 2–3: The UIR Features and the Extended Red Emission

We now have good infrared observations of other galaxies and of the diffuse ISM emission

in our own galaxy. In both cases the near-infrared to middle-infrared emission (say from 2 to 25 μm) is usually dominated by the *Unidentified Infrared Emission* features. These are seen to be strong in reflection nebulae and dusty HII regions, and since a number of the wavelengths of these features correspond to bond resonances in aromatic organic compounds it is clear that these features are due to very small grains/large molecules formed from carbon rings. The details of this have been debated for some years. The simplest such compounds are *polycyclic aromatic hydrocarbons* or PAHs, just benzene-like molecules. There are reasons to think that the molecules are a bit more chemically complex, so there are competing hypotheses such as *hydrogenated aromatic compounds*, called HACs, which are essentially the same type of molecule with additional hydrogen atoms added. Another such hypothesis is very small coal particles: that is small grains of made from a random collection of small “bricks” which have layers of aromatic rings material and a size of about 10 to 20 Å, held together by functional groups such as CH, CH₂, COH, or oxygen bridges which connect the many bricks into one grain. It is surprising how well simple coal dust matches many aspects of the infrared emission in the UIR features. (Of course, since coal on Earth is biological in origin the grains in space presumably have some other origin.) Yet another is *quenched carbonaceous composite* or QCCs which refers to a material produced in a plasma discharge from a gas containing hydrogen and carbon. All of these materials are reasonably similar in overall chemical makeup although the exact chemistry is different in each case.

Related to the UIR features is an emission in the red part of the optical spectrum, roughly from 5300 to 7500 Å with a peak at around 6400 Å, which is seen in reflection nebulae, HII regions, and planetary nebulae. This emission is thought to be due to some type of luminescence in the same grains that produce the UIR features. What this means is that the material is excited by blue or UV photons and that this excites various internal modes—probably vibrational—which radiate energy in the various features that we observe. Since each electronic level has many associated vibrational modes in a moderately large molecule, for any excited electronic state there are likely to be vibrational states of other electronic states with almost the same energy, and the molecule will then be able to move to other vibrational states—and as a by-product to other electronic states—quite readily. Then the resulting spectrum becomes quite complicated. especially when the number of accessible levels is very large. Rather than having a series of discrete lines, the molecule emits in many overlapping bands to form an effective continuum. That continuum is likely what we observe in the ISM as this optical continuum.

That idea is primarily due to the observation of the Red Rectangle, an extreme object in which this *extended red emission* dominates the optical spectrum. The object is a star,

HD 44179, surrounded by a bipolar reflection nebula that produces the ERE. The ERE also has some narrow emission features that correspond to the *diffuse interstellar bands* (DIBs), a large set of weak bands that occur in the ISM. The diffuse bands are not due to atoms since no individual lines are seen, but consist of hundreds of narrow bands (1 to 2 Å wide, which is much wider than absorption lines formed in the ISM since the pressure is very low and the kinetic temperature can also be small) in the optical through the UV.

Figure 46 shows a comparison of the emission from the reflection nebula in the red rectangle and that from the star itself. This figure is taken from G. D. Schmidt, M. Cohen, & B. Margon (1980; ApJ, **230**, L133). The stellar spectrum was taken with a small aperture centered on the star, while the spectrum of the nebula was taken at a point offset from the star. For comparison with the reflection nebula spectrum the stellar spectrum has been scaled down by a factor of 1300 to match at 5000 Å. One sees that the reflected spectrum is slightly bluer than the stellar spectrum, which is caused by the scattering efficiency of the grains going up somewhat with the frequency of the light. In the red part of the spectrum the ERE shows up quite clearly from about 5400 Å to the end of the spectrum.

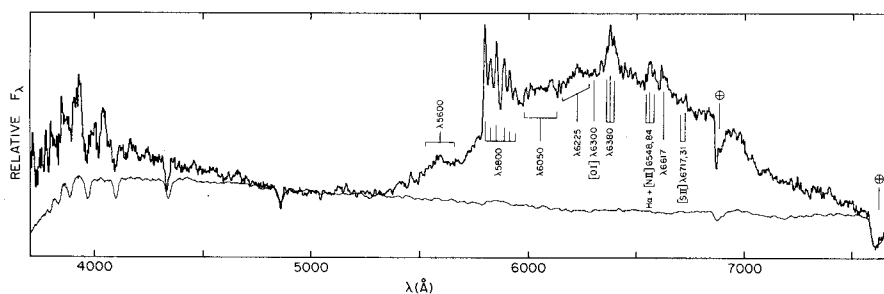


Figure 46—The optical spectrum from a position in the reflection nebulosity around star HD 44179, the Red Rectangle, compared to the scaled stellar spectrum. The reflected light is similar to the stellar spectrum in the blue end but there is the ERE component in the long wavelength part of the spectrum. This is copied from Schmidt, Cohen, and Margon (1980).

There are some individual lines in the ERE itself, particularly from 5800 to 5900 Å. These are not normally seen in other objects, where the ERE is much weaker than it is in the Red Rectangle. It can be demonstrated that the red emission is not due to scattering as such, because the stellar spectrum does not show a dip in the 5500 to 8000 Å wavelength range. The stellar spectrum does suffer from extinction in the surrounding nebula which can be observed by comparing it to that of an unreddened star of the same type.

I show an HST image of the source in Figure 47. This image is taken in a broad-band filter centered at 8200 Å, in the far-red part of the spectrum. The image shown is a false-

colour image. There is a central nebulosity divided by a dust lane, which is where the star is. There is also a fainter bipolar nebula which is hour-glass shaped. The nebula has a size of 6 by 4 arcseconds on the sky.

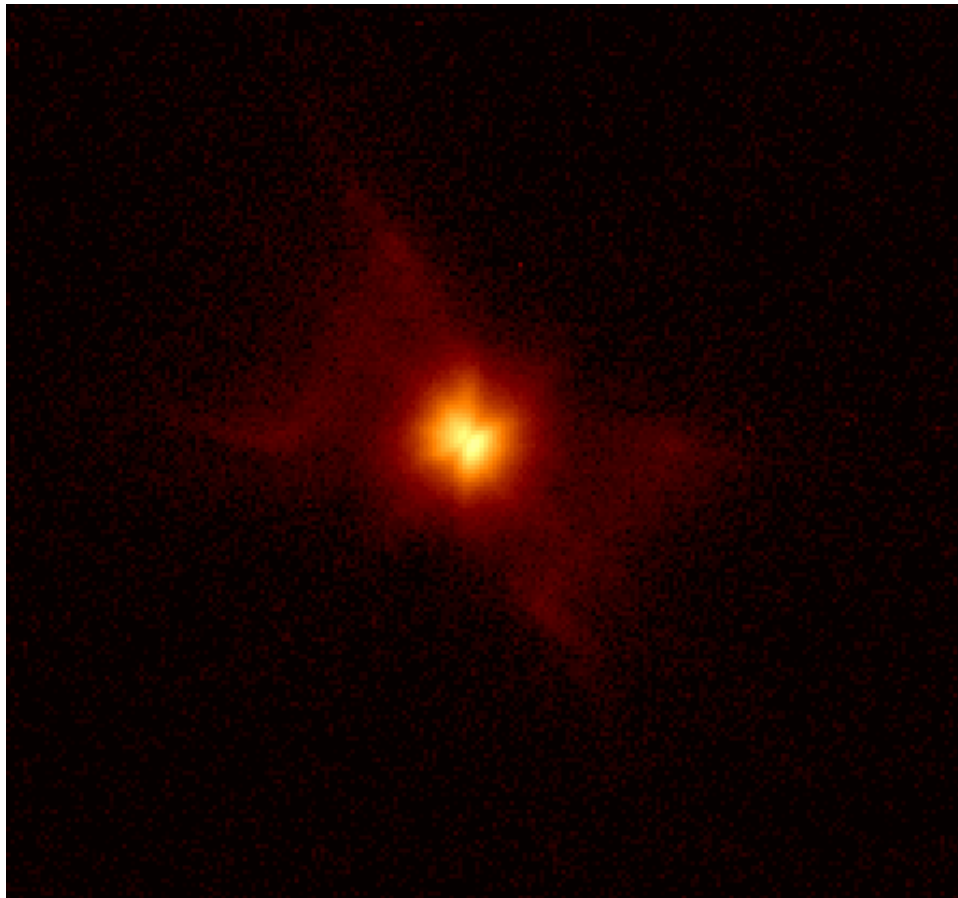


Figure 47—An HST image of the Red Rectangle in a broad-band filter in the red part of the optical spectrum, around 8000 Å. There is a bright central region, bisected by a dark dust lane, and an hour-glass shaped bipolar nebula beyond that.

In the infrared the Red Rectangle shows strong UIR features which implies that all these aspects of the ISM emission and absorption come from a common source. It is thus thought that the UIR features, the ERE, and the DIBs all come from some type of small carbon grains. Laboratory studies of PAHs and related molecules support this general picture and suggest that if 10% of the available carbon in the Red Rectangle are in the form of PAHs or related molecules then the star provides them with enough energy to produce the ERE.

The small grains/large molecules which make the UIR features are also now thought to be responsible for the long wavelength diffuse emission at wavelengths less than 60 μm . In this case, large grains would be too cool to produce this emission, given the estimated

radiation field intensity of the general ISM. As mentioned above, the T_d value of a grain may not give a good picture of its emission when the radiation field gets too diffuse and the grain is small. The intensity of the various UIR features in the ISM along with the dust continuum can be matched quite well by the quantum heating models.

Section 2–4: Putting It All Together

People have tried to combine all these observations and make general models to match the ISM extinction curve as well as the individual properties I have discussed. The most successful such model is that of J. S. Mathis, W. Rumble, and K. H. Nordsieck (1977; *ApJ*, **217**, 425). They use silicate grains to match the infrared features and to provide some of the optical extinction. There are also some small silicate grains to produce some of the far-UV extinction. To match the 2200 Å bump they use graphite grains, which also provide some of the optical extinction. Their model matches the average ISM extinction curve, the strengths of the various features, and the depletions observed in the ISM. The silicate particles are primarily responsible for the polarization in this model, since they have a high albedo—that is, a large scattering to absorption ratio—in the optical range. The graphite grains have a low albedo.

In this model the optical extinction is 60% due to graphite grains and 40% due to silicate grains. Graphite grains dominate at the 2200 Å bump and silicate grains dominate in the far-UV from 2000 Å down to about 1000 Å after which the two contribute about equally.

To make this work a size distribution has to be assumed, since the Q values vary with a at a given λ . The size distribution they derived is

$$N(a) = N(a_0) \left(\frac{a}{a_0} \right)^{-2.5} \quad (5.23)$$

with a lower size limit of 100 Å and an upper size limit of about 2500 Å. The lower limit value is not very constrained by the available data. It must be 100 Å or less to have enough small grains to produce the proper amount of far-UV extinction. This size distribution is more commonly given as

$$dN(a) = AN_H a^{-3.5} da \quad (5.24)$$

where N_H is the hydrogen column density and A is a constant. This size distribution matches the long wavelength ($\lambda \geq 100 \mu\text{m}$) emission of the general ISM fairly well but fails at shorter infrared wavelengths. If the size distribution extends below 100 Å down to of order 50 Å or less then these problems may be resolved. A good review of this is given by P. A. Aannestad (1989; *Evolution of Interstellar Dust and Related Topics*, ed. A. Bonetti, J. M. Greenberg, & S. Aiello, p. 121).

The size distribution deduced by Mathis *et al.* (1977) is taken to be the standard one for the ISM in general. Since the grain mass goes as a^3 , the distribution of masses with a goes as $a^{-1/2}$. That means that there are not only many more small grains, but that more of the mass is in the small grains than in the large ones.

Since the large grains are much rarer than the small ones in this picture, there could be a population of large grains without their causing much in the way of observational consequences. There has been some speculation about grains of sizes $a > 1 \mu\text{m}$ in the ISM, but there has been no agreement on this point.

Section 3: Dust in Different Phases of the ISM

The dust grains in the entire ISM of the Galaxy, or in other galaxies, span a wide range in temperature. Which part of the dust population is important in a given wavelength range depends on where the peak of the emission curve matches a given wavelength. The emission is not the same as for a blackbody since the $Q_{\text{abs}}(\lambda)$ function of the grains at long wavelength alters the emission. The standard picture of Q_{abs} at far-infrared wavelengths is that it varies as $\lambda^{-1.8}$.

Section 3-1: Hot Grains ($T > 60 \text{ K}$)

From 10 to 50 μm the dust emission we observed comes from grains of temperature 60 K or higher. Part of this emission is definitely due to small grains since the UIR features can be observed from the diffuse ISM. Some of the emission is due to gas near HII regions or other sources of radiation. The infrared spectra of galaxies as a whole in the 8 to 23 μm wavelength range are very similar to those of reflection nebulae or those of compact HII regions. They show the UIR features on a background continuum, and the UIE features are normally not that strong. However in M82, which is a star-burst galaxy, the UIR features are quite strong in the IR spectrum. The same sort of thing is seen in other star-burst galaxies, such as Arp 229. The dust continuum indicates temperatures of order 100 K to 150 K for the hot dust.

What seems to happen is that the large rate of star formation produces a strong ISM radiation field and the UIR producing grains are heated more efficiently giving stronger UIR bands. In more normal galaxies the emission in the 10 to 40 μm wavelength range is mostly associated with HII regions, and seems to come from the area just beyond the ionized region where there is plenty of UV radiation to heat any dust that is nearby. Where maps can be made, the emission near 10 μm comes from areas of galaxies where we see HII regions. Studies of the Orion Nebula have shown that its UIR emission definitely comes

from outside the ionized region, which indicates that the small grains making these features are destroyed by the UV radiation and electron bombardment inside the ionized region. This is probably generally true in the Galaxy and in other galaxies. Thus there is a strong correlation between this dust emission and star formation.

Section 3–2: Warm Dust: $T \approx 50$ K

Many galaxies have infrared emission which peaks around $60 \mu\text{m}$. The dust that produces this emission has a temperature of 25 to 60 K or so, and I take 50 K as a representative number. There is still some component from the small grains producing the UIR bands, but most of the emission is from somewhat larger grains. Here the dust emission is not associated with star formation regions. This emission occurs in normal elliptical galaxies and the earlier type spiral galaxies where star formation is either weak or absent. This dust component is found wherever the ISM radiation field is strong enough to heat the grains to such temperatures, and so even in an old stellar population this emission is seen as long as the stellar density is high enough, such as in the bulges of Sa or S0 type spirals and elliptical galaxies.

At the low end of the temperature range this dust produces the emission at around $100 \mu\text{m}$. Since the *Infrared Astronomical Satellite* carried out an all-sky survey at 60 and $100 \mu\text{m}$ and there has been no other such survey at long wavelengths, the study of the infrared properties of galaxies is strongly biased to this component and the hotter component of the dust. Individual galaxies and some parts of the Galaxy have been observed at longer wavelengths, so we know that still cooler dust does exist in the ISM and radiates a significant amount of energy

Section 3–3: Cool Dust: $T \approx 15$ K

Dust grains with temperatures from 10 to 25 K radiate mostly in the sub-mm wavelength range. For some time it was not clear whether this dust was common or whether the observations available could be fit by hotter grains and a steeper $Q_{\text{abs}}(\lambda)$ function. It turns out that the dust in this temperature range accounts for a large fraction of the total dust mass in the ISM. It seems to always be associated with molecular gas, and so it is mostly in the giant molecular clouds.

For a few galaxies there have been maps made in CO and at $1300 \mu\text{m}$ where the cool dust dominates. The resulting maps are extremely similar in their features, whereas the neutral H maps look different.

This dust is also responsible for most of the dust emission seen by COBE for the Galaxy. The COBE beam size of 7° was far too large for study of anything but the overall structure

of the emission. The mean spectrum from the FIRAS instrument indicates a temperature of around 20 K or so for greybody grains.

Section 3–4: Very Cold Dust?

It is possible that there is dust cooler than 10 K in the ISM. If so it probably cannot have a large mass in view of the COBE results. Such dust could be present in the heart of molecular clouds, shielded from radiation by the surrounding material, or far from the Galactic disk. So far there is no concrete observation of this type of dust.

Section 4: Conclusion

All this discussion has in one sense only scratched the surface of the topic of dust in the ISM. There are many unknowns in the study of the dust, and I hope that some of the upcoming satellite missions that are intended to observe in the far-infrared and sub-mm wavelength ranges will fill in a number of these gaps. I think that there are certainly four areas at least which need more basic data:

- 1) Composition of dust grains—While the Mathis *et al.* (1977) grain model is able to generally reproduce the dust extinction curve, it is probably wrong in its fitting of the 2200 Å feature. We do know from various observations that the dust in the ISM includes silicates and carbonaceous grains, but we are in the dark about many details. We need to figure out what form the carbon grains take (coal?) and what their relation to the UIR features is. We have now many observations of the infrared emission from these grains and should be able to deduce something of their properties. It may be that studies of meteoritic and cometary material thought to be derived from the formation of the solar system will be our guide in this area.
- 2) Heating of the dust grains—We know that HII regions and regions of star formation heat the dust that is nearby. However we also know from observations of reflection nebulae that the grains can absorb radiation from cooler stars. Many reflection nebulae that show the UIR features and reasonable amounts of infrared emission are illuminated by intermediate type stars such as G-type giants and supergiants. This is something which has not been given much attention in the past, but it should tell us about the grain absorption and scattering properties in the blue to the middle UV. Many substances have strong features there, so this can help us trace the different possible grain materials.
- 3) Dust features—Prior to the recent *Infrared Space Observatory* mission there had been only limited observations of the dust emission at long wavelengths. We would really like detailed spectral information from different dust environments to see what information

we can gather about the dust grains. The 10 and 18 μm silicate features have been known for a long time, but other features have not been found as readily. We know that there should be features due to ices and other possible grain coatings, and we hope that we can find features due to other molecular bonds in the grains. These can be studied in late-type stars, which are one important source of the original dust grains, in dusty HII regions, and in molecular clouds generally. It is to be hoped that we can get quantitative comparisons of the grains in these various environments.

- 4) Grain evolution—Clearly the ISM is a fairly hostile medium for the grains, and so grains should undergo physical changes with time due to shocks, the UV radiation, and chemical reactions with the gas. Attempts have been made to model the “life history” of dust grains in the ISM. However finding clear observational tests of these models has not been easy. If we have better data from the infrared and sub-mm wavelength ranges we can try to trace chemical species and the reactions which may lead to the formation of the dust grains, or those that result from the breakdown of existing grains. Finding out more about dust from comets also will help us understand the grains in the ISM.